Articles

Linkage Isomerism in Complexes of *o*-Xylylene: Density Functional Study of the Structure and Bonding in *endo*- and *exo*-$Ru(PH_3)_3$(*o*-xylylene)

John E. McGrady,[†] Robert Stranger,*[,†] Mark Bown,[‡] and Martin A. Bennett[‡]

Department of Chemistry, Faculties, The Australian National University, Canberra, ACT 0200, Australia, and Research School of Chemistry, The Australian National University, Canberra, ACT 0200, Australia

Received February 5, 1996[⊗]

The bonding in η^4 complexes of butadiene (C_4H_6) and *o*-xylylene (C_8H_8) with zerovalent ruthenium is examined using density functional theory. The ruthenium−butadiene bond is shown to be stabilized principally by charge transfer from the metal to the ligand, as a result of which the central C−C bond is contracted relative to that in the free ligand. Back-bonding is further enhanced by a rotation of the substituents at the terminal carbon atoms, resulting in a stabilization of the ligand LUMO and also enhanced overlap of metal and ligand-based orbitals. The major features of the bonding in butadiene complexes are extended to the *o*-xylylene ligand, which contains two fused butadiene fragments and, hence, two distinct η^4 coordination sites. The *exo* isomer of $Ru(PH_3)_3$(*o*-xylylene) is found to be more stable than its *endo* counterpart, principally due to an aromatization of the six-membered ring when coordination occurs at the *exo* site. In addition, the stabilizing influence of the rotation of the terminal carbon atoms is less pronounced in the *endo* isomer, due to the steric constraints of the six-membered ring.

Downloaded by CARLI CONSORTIUM on June 30, 2009
Published on January 1, 1996 on http://pubs.acs.org | doi: 10.1021/om9600755

Introduction

Complexes of 1,3-butadiene with a wide variety of transition metals are known.[1] The most extensively studied group is that containing the iron tricarbonyl fragment, $Fe(CO)_3$, which is often used as a protecting group for dienes in organic synthesis because the complexes are stable under a wide variety of reaction conditions.[2] Complexes of ruthenium are also well documented,[3,4] and examples are known where the diene coordinates in a η^4 fashion in both the *cisoid* (Figure 1, I) and, less commonly, *transoid* (Figure 1, II) conformations.[5,6] Both conformations have been identified for complexes of Ru^{II}, but only the *cisoid* conformation is known for zerovalent ruthenium or, indeed, any other zerovalent metal.

The highly reactive unsaturated molecule quinodimethane (*o*-xylylene) (III) has been stabilized by transition metal centers in a variety of bonding modes.[7] The *o*-xylylene molecule may be regarded as containing two distinct butadiene sites, and transition metals are known to coordinate in a η^4 fashion at either the *endo* (IV) or *exo* (V) sites. In some cases, both sites may be coordinated simultaneously (VI), with the metal atoms in either *syn*[8] or *anti*[7,9] configurations with respect to the plane of the *o*-xylylene. Coordination of an *o*-

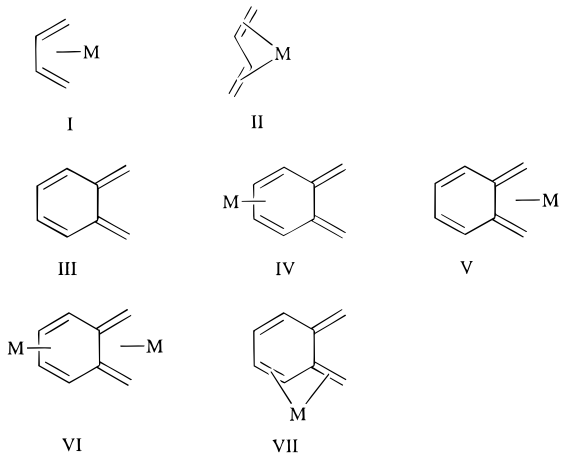

Figure 1. Coordination modes of butadiene and *o*-xylylene.

[†] Department of Chemistry.
[‡] Research School of Chemistry.
[⊗] Abstract published in *Advance ACS Abstracts,* June 1, 1996.

(1) Collman, J. P.; Hegedus, L. S.; Norton, J. R.; Finke, R. G. *Principles and Applications of Organotransition Metal Chemistry,* 2nd ed.; University Science Books: Mill Valley, CA, 1987.
(2) Hegedus, L. S. *Transition Metals in the Synthesis of Complex Organic Molecules*; University Science Books: Mill Valley, CA, 1994.
(3) Bennett, M. A. In *Comprehensive Organometallic Chemistry II*; Abel, E. W., Stone, F. G. A., Wilkinson, G., Eds.; Pergamon: Oxford, U.K., 1995; Vol. 7, pp 449−455.
(4) Bennett, M. A.; Khan, K.; Wenger, E. In *Comprehensive Organometallic Chemistry II*; Abel, E. W., Stone, F. G. A., Wilkinson, G., Eds.; Pergamon: Oxford, U.K., 1995; Vol. 7; pp 483−485, 506−509.
(5) Benyunes, S. A.; Day, J. P.; Green, M.; Al-Saadoon, A. W.; Waring, T. L. *Angew. Chem., Int. Ed. Engl.* **1990**, *29*, 1416−1417.
(6) Ernst, R. D.; Melendez, E.; Stahl, L.; Ziegler, M. L. *Organometallics* **1991**, *10*, 3635−3642.
(7) Bennett, M. A.; Bown, M.; Goh, L. Y.; Hockless, D. C. R.; Mitchell, T. R. B. *Organometallics* **1995**, *14*, 1000−1007.
(8) Mena, M.; Royo, P.; Serrano, R.; Pelllinghelli, M. A.; Tiripicchio, A. *Organometallics* **1988**, *7*, 258−262.
(9) Hull, J. W., Jr.; Mann, C.; Gladfelter, W. L. *Organometallics* **1992**, *11*, 3117−3121.

S0276-7333(96)00075-1 CCC: $12.00 © 1996 American Chemical Society

xylylene ligand (VII) in a *transoid* fashion is, however, unknown. Although a variety of different *endo*- and *exo*-coordinated complexes have been structurally characterized, the first isomeric pair of *o*-xylylene complexes, *endo*- and *exo*-Ru(PMe_2Ph)$_3$(*o*-xylylene), was reported only recently.[7,10,11] The co-existence of both isomers raises questions about the electronic factors which determine the relative stability of the two.

In recent years, density functional theory (DFT) has been used successfully to provide information about the structures and energetics of a variety of organometallic compounds and transformations.[12] In this paper, we use DFT to determine the relative stabilities of the *endo* and *exo* isomers of Ru(PH_3)$_3$(*o*-xylylene). In addition, we examine the features of the bonding which give rise to the distinct nonplanarity of the six-membered ring in the *endo* isomer. To a first approximation, *o*-xylylene may be regarded as two fused butadiene fragments. Accordingly, we first analyze in detail the structure and bonding in a model ruthenium−butadiene complex, Ru(PH_3)$_3$(C_4H_6), and then extend the basic conclusions to the two isomers of Ru(PH_3)$_3$(*o*-xylylene). Aspects of the bonding in butadiene complexes have been described previously using both extended Hückel[13] and *ab initio* SCF molecular orbital theory.[14] As in simple olefin complexes, both donation of charge from the ligand to the metal and also metal-to-ligand back-bonding contribute to the overall stability of the complex. Through a detailed analysis of the interaction between the metal fragment (Ru(PH_3)$_3$) and the ligand (butadiene or *o*-xylylene), it is possible for the first time to quantify the relative importance of the two bonding mechanisms.

Computational Details

All calculations described in this paper are based on approximate density functional theory and were performed using the Amsterdam Density Functional (ADF) program version 2.0.1 developed by Baerends and co-workers.[15] The valence orbitals of the main group elements were expanded in double-ζ Slater-type basis sets, augmented with a single 2p-type polarization function for hydrogen and a single d function for carbon and phosphorus. The orbitals of ruthenium were represented by a triple-ζ basis.[16] An auxiliary set of s, p, d, f, and g Slater functions was used to fit the molecular electron density.[17] Electrons in orbitals up to and including 1s (C), 2p (P), and 4p (Ru) were considered as cores and treated using the frozen core approximation. Geometries of all species were optimized using the local exchange-correlation potential of Vosko, Wilk, and Nusair.[18] Interaction energies were calculated at the optimized geometries using the local density approximation with the gradient corrections of Becke[19] and Perdew.[20] Interaction energies were decomposed according to the generalized transition state approximation.[21] Geometries were optimized within C_s symmetry in all cases, using the gradient algorithm of Versluis and Ziegler.[22]

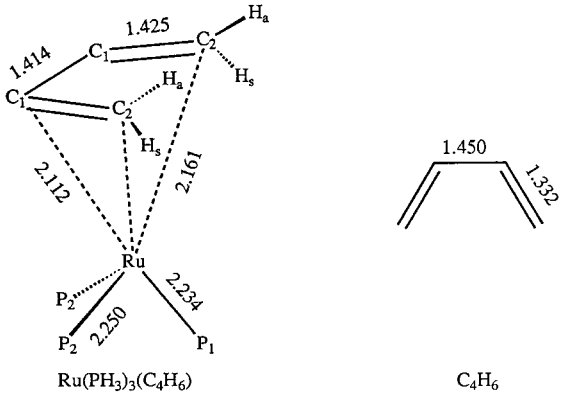

Figure 2. Optimized bond lengths (Å) of *cis*-butadiene, C_4H_6, and Ru(PH_3)$_3$(C_4H_6).

Results and Discussion

Electronic and Molecular Structure of Ru(PH_3)$_3$(C_4H_6). The optimized geometry of Ru(PH_3)$_3$(C_4H_6) is shown in Figure 2, along with that of the free ligand, C_4H_6. In the optimization procedure, the symmetry-unique phosphine group was placed over the open face of the butadiene ligand, in accord with the experimentally determined structures of the majority of known ML_3(butadiene) complexes.[23] The reasons for the preference for this conformation over the alternative C_s structure, where the unique phosphine lies over the central C_1-C_1 bond, have been explored elsewhere[13b] and will not be discussed here. The optimized structure conforms to the square pyramidal geometry typical of ML_3(butadiene) complexes, with the two C=C double bonds occupying equatorial positions. The axial Ru−P

Downloaded by CARLI CONSORTIUM on June 30, 2009
Published on July 1, 1996 on http://pubs.acs.org | doi: 10.1021/om960077b

(10) Bennett, M. A.; Goh, L. Y.; McMahon, I. J.; Mitchell, T. R. B.; Robertson, G. B.; Turney, T. W.; Wickramasinghe, W. A. *Organometallics* **1992**, *11*, 3069−3085.

(11) Chappell, S. D.; Cole-Hamilton, D. J.; Galas, A. M. R.; Hursthouse, M. B. *J. Chem. Soc., Dalton Trans.* **1982**, 1867−1871.

(12) (a) Ziegler, T. *Chem. Rev.* **1991**, *91*, 651−667. (b) Ziegler, T. *Pure Appl. Chem.* **1991**, *63*, 873−878. (c) Branchadell, V.; Deng, L.; Ziegler, T. *Organometallics* **1994**, *13*, 3115−3119. (d) Woo, T. K.; Fan, L.; Ziegler, T. *Organometallics* **1994**, *13*, 2252−2261. (e) Bickelhaupt, F. M.; Ziegler, T.; Schleyer, P. v. R. *Organometallics* **1995**, *14*, 2288−2296. (f) Fan, L.; Krzywicki, A.; Somogyvari, A.; Ziegler, T. *Inorg. Chem.* **1994**, *33*, 5287−5294. (g) Ziegler, T. *Can. J. Chem.*, **1995**, *73*, 743−761.

(13) (a) Mingos, D. M. P. In *Comprehensive Organometallic Chemistry II*; Wilkinson, G., W., Stone, F. G. A., Abel, E. Eds.; Pergamon: Oxford, U.K., 1982; Vol. 3, pp 60−67. (b) Mingos, D. M. P. *J. Chem. Soc., Dalton Trans.* **1977**, 20−25. (c) Mingos, D. M. P.*Adv. Organomet. Chem.* **1977**, *15*, 1−51. (d) Hoffmann, R.; Hofmann, P. *J. Am. Chem. Soc.* **1976**, *98*, 598−604. (e) Albright, T. A.; Hofmann, P.; Hoffmann, R. *J. Am. Chem. Soc.* **1977**, *99*, 7546−7557. (f) Yasuda, H.; Tatsumi, K.; Okamoto, T.; Mashima, K.; Lee, K.; Nakamura, A.; Kai, Y.; Kanehisa, N.; Kasai, N. *J. Am. Chem. Soc.* **1985**, *107*, 2410−2422. (g) Harlow, R. L.; Krusic, P. J.; McKinney, R. J.; Wreford, S. S. *Organometallics* **1982**, *1*, 1506−1513. (h) Tatsumi, K.; Yasuda, H.; Nakamura, A. *Isr. J. Chem.* **1983**, *23*, 145−150.

(14) Connor, J. A.; Derrick, L. M. R.; Hall, M. B.; Hillier, I. H.; Guest, M. F.; Higginson, B. R.; Lloyd, D. R. *Mol. Phys.* **1974**, *28*, 1193−1205.

(15) (a) Baerends, E. J.; Ellis, D. E.; Ros, P. *Chem. Phys.* **1973**, *2*, 42−51. (b) Baerends, E. J.; Ros, P. *Chem. Phys.* **1973**, *2*, 52−59. (c) Baerends, E. J.; Ros, P. *Int. J. Quantum Chem.* **1978**, *S12*, 169−190.

(16) Krijn, J.; Baerends, E. J. *Fit Functions in the HFS Method*; Internal Report; Free University of Amsterdam: Amsterdam, The Netherlands, 1984.

(17) Vernooijs, P.; Snijders, G. J.; Baerends, E. J. *Slater Type Basis Functions for the Whole Periodic System*; Internal Report; Free University of Amsterdam: Amsterdam, The Netherlands, 1981.

(18) Vosko, S. H.; Wilk, L.; Nusair, M. *Can. J. Phys.* **1980**, *58*, 1200−1211.

(19) Becke, A. D. *Phys. Rev. A* **1988**, *38*, 3098−3100.

(20) Perdew, J. P. *Phys. Rev. B* **1986**, *33*, 8822−8824.

(21) (a) Ziegler, T.; Rauk, A. *Theor. Chim. Acta* **1977**, *46*, 1. (b) Ziegler, T.; Rauk, A. *Inorg. Chem.* **1979**, *18*, 1558−1565. (c) Ziegler, T.; Rauk, A. *Inorg. Chem.* **1979**, *18*, 1755−1759.

(22) Versluis, L.; Ziegler, T. *J. Chem. Phys.* **1988**, *88*, 322−328.

(23) Deeming, A. J. In *Comprehensive Organometallic Chemistry II*; Wilkinson, G. W., Stone, F. G. A., Abel, E., Eds.; Pergamon: Oxford, U.K., 1982; Vol. 4, pp 449−459 and references therein.

(24) (a) Cotton, F. A.; Day, V. W.; Frenz, B. A.; Hardcastle, K. I.; Troup, J. M. *J. Am. Chem. Soc.* **1973**, *95*, 4522−4528. (b) Herbstein, F. H.; Reisner, M. G. *Acta Crystallogr.* **1977**, *B33*, 3304−3317. (c) Cotton, F. A.; Troup, J. M. *J. Organomet. Chem.* **1974**, *77*, 369−379.

(25) (a) Mills, O. S.; Robinson, G. *Acta Crystallogr* **1963**, *16*, 758−761. (b) Henderson, G. L.; Roehrig, M. A.; Wikrent, P.; Kukolich, S. G. *J. Phys. Chem.* **1992**, *96*, 8303−8306. (c) Kukolich, S. G.; Roehrig, M. A.; Henderson, G. L.; Wallace, D. W.; Chen, Q.-Q. *J. Chem. Phys.* **1992**, *97*, 829−831.

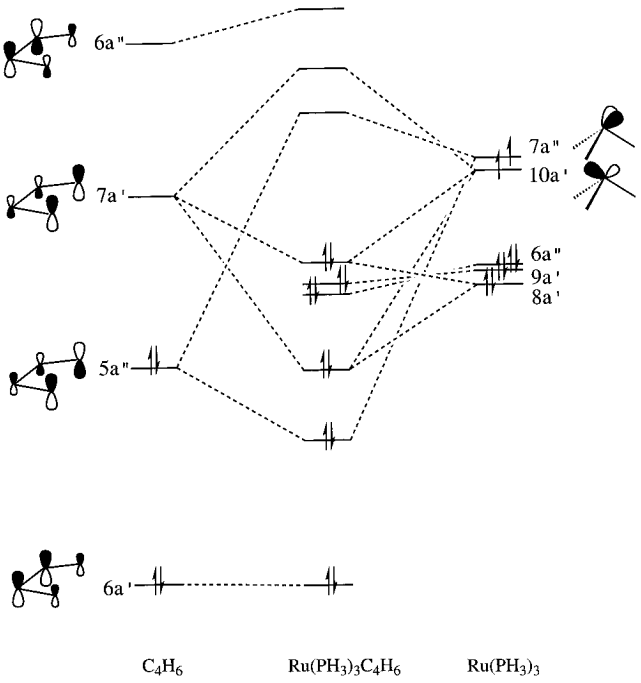

Figure 3. Molecular orbital diagram summarizing the interaction of a Ru(PH$_3$)$_3$ fragment with *cis*-butadiene.

bond, Ru−P$_1$, is marginally shorter than its equatorial counterparts, consistent with the absence of a ligand in the *trans* position. In terms of the following discussion of *o*-xylylene complexes, the most significant features of the structure relate to the coordination-induced distortions in the butadiene ligand.

First, the central C$_1$−C$_1$ bond contracts significantly upon coordination, while the C$_1$−C$_2$ bonds lengthen. Second, the hydrogen atoms at the terminal carbons (C$_2$) undergo a disrotatory motion, the dihedral angles defined by C$_1$−C$_1$−C$_2$−H$_a$ and C$_1$−C$_1$−C$_2$−H$_s$ being 45 and 190°, respectively (compared to values of 0 and 180°, respectively, for a strictly coplanar ligand). As a result, the *anti* hydrogens (H$_a$) lie approximately 0.7 Å above the C$_4$ plane while the hydrogens in the *syn* position (H$_s$) are displaced 0.15 Å below it. Smaller distortions occur at the inner carbon atoms (C$_1$), also displacing the protons slightly below the plane defined by the carbon framework. Both the contraction of the central C$_1$−C$_1$ bond and the disrotatory motion of the methylene protons are highly characteristic of coordinated butadienes.

A qualitative molecular orbital diagram summarizing the major interactions between the frontier orbitals of C$_4$H$_6$ and Ru(PH$_3$)$_3$ fragments is shown in Figure 3. The HOMO of C$_4$H$_6$, 5a″, is bonding with respect to C$_1$−C$_2$ but antibonding with respect to the central C$_1$−C$_1$ axis. In contrast, the LUMO, 7a′, is antibonding with respect to C$_1$−C$_2$ but bonding with respect to C$_1$−C$_1$. The remaining two orbitals of the butadiene π system, 6a′ and 6a″, are either too low (6a′) or too high (6a″) in energy to contribute significantly to the Ru−butadiene bonding and will not be considered further. The frontier orbital domain of the neutral Ru(PH$_3$)$_3$ fragment consists of three approximately degenerate filled orbitals (8, 9a′, 6a″), which are essentially Ru−P nonbonding, and two singly occupied Ru−P σ antibonding orbitals (10a′, 7a″) at higher energy.

Within the a″ representation, the major bonding interaction is between the HOMO of C$_4$H$_6$ (5a″) and the 7a″ orbital of Ru(PH$_3$)$_3$, resulting in a *destabilization* of the metal-based orbital. In a′ symmetry, the 10a′ orbital of Ru(PH$_3$)$_3$ is *stabilized* by a bonding interaction with the LUMO of C$_4$H$_6$, 7a′. Thus the first consequence of the interaction of a Ru(PH$_3$)$_3$ fragment with butadiene is a transfer of a single electron from the metal-based 7a″ orbital to 10a′, resulting in a Ru(PH$_3$)$_3$ valence configuration of (a′)^{20}(a″)^{12}. From this reference point, the synergic nature of the Ru−butadiene bonding becomes clear. Interactions within a″ symmetry result in depopulation of the C$_4$H$_6$ HOMO and, therefore, constitute a transfer of charge from ligand to metal. In contrast, the interaction of the a′ orbitals results in a population of the ligand LUMO and hence a transfer of charge in the opposite direction. The qualitative nature of this bonding scheme has been described elsewhere,[13,23] but with the aid of the generalized transition state method, we are now in a position to quantify the relative importance of metal-to-ligand and ligand-to-metal charge transfer in stabilizing the Ru−butadiene bond.

Within the generalized transition state approximation,[21] the formation of the metal−ligand bond is conceptually broken down into three distinct steps. First, the two fragments are distorted from their equilibrium geometries and electronic configurations to those characteristic of the fragment in the complex itself. The preparation energy, ΔE_{prep}, associated with this process is dominated by the energy required to distort the butadiene ligand to the geometry it adopts when coordinated, but also includes a smaller term associated with the formation of the (a′)^{20}(a″)^{12} valence state of the Ru(PH$_3$)$_3$ fragment from the (a′)^{19}(a″)^{13} ground state. In the second step, the two fragments are brought up to their equilibrium bonding geometry while maintaining the electron density distribution characteristic of the isolated fragments. The energy associated with this step, ΔE_{steric}, contains terms due to electrostatic forces between the fragments and also the destabilizing two-center-four-electron repulsive interactions associated with the overlap of fully occupied orbitals. Finally, the occupied and virtual orbitals of the two fragments are allowed to interact, permitting the electron density to relax to the electronic ground state. The orbital interaction term, ΔE_{oi}, associated with this final step may be further decomposed into separate terms for each irreducible representation of the group. This final point is most significant, because, as noted above, metal-to-ligand and ligand-to-metal contributions to the overall bond strength are contained primarily within the a′ and a″ representations, respectively. The fragment approach therefore allows us to assess the energetic contribution of both forward- and back-bonding mechanisms to the overall stability of the complex. Similar procedures have been utilized to analyze the bonding in complexes of other potentially π back-bonding ligands such as C$_2$H$_4$,[21b] CO and N$_2$.[21c]

The various components of the Ru(PH$_3$)$_3$ - C$_4$H$_6$ bonding energy are summarized in Table 1, along with the total energy, ΔE_{tot}, defined as

$$\Delta E_{tot} = \Delta E_{prep} + \Delta E_{steric} + \Delta E_{oi}$$

The decomposition of the ΔE_{oi} term clearly illustrates that metal-to-ligand back-bonding is the dominant bonding force, the energy associated with interactions

Downloaded by CARLI CONSORTIUM on June 30, 2009
Published on July 1, 1996 on http://pubs.acs.org | doi: 10.1021/om9600235

Table 1. Components of the Total Energy and Mulliken Population Analyses for Full and Partially Optimized Structures of $Ru(PH_3)_3(C_4H_6)$

Energy/kcal mol^{-1}

	full optimization	partial optimization
ΔE_{prep}	38.06	8.70
ΔE_{st}	103.19	88.47
ΔE_{oi}		
a′	−147.15	−109.97
a″	−69.71	−49.82
corr[a]	4.88	4.51
ΔE_{tot}	−70.73	−58.11

Fragment Populations

	$Ru(PH_3)_3$	C_4H_6	$Ru(PH_3)_3$	C_4H_6
a′	18.44	13.56	18.78	13.22
a″	12.30	9.70	12.20	9.70
tot.	30.74	23.26	31.08	22.92

[a] Correction term accounting for the incomplete fit provided by the auxiliary functions.

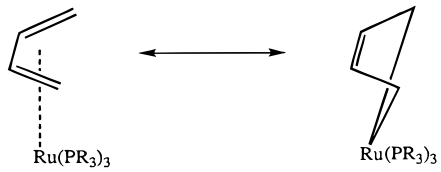

1-4η-diene enediyl

Figure 4. 1−4-η−Diene and enediyl canonical forms of $Ru(PH_3)_3(C_4H_6)$.

in the a′ representation being more than twice as large as the term in a″. The dominance of back-bonding is confirmed by the total fragment populations, also summarized in Table 1. The process of bond formation results in a transfer of 1.26 electrons from the metal [initially $(a')^{20}(a'')^{12}$] to the ligand [$(a')^{12}(a'')^{10}$], consisting of a net transfer of 0.30 electrons from ligand to metal (in a″), and a back-donation of 1.56 electrons in the opposite direction (in a′).

Having established a quantitative description of the metal−ligand bonding, we can now examine the origin of the distortions of the coordinated butadiene fragment described above. The contraction of the central C_1-C_1 bond has been noted in a wide variety of metal−butadiene complexes[22,23] and traced to the partial population of the LUMO of C_4H_6, 7a′, in the coordinated ligand (see Figure 3).[13a] This orbital is antibonding with respect to C_1-C_2, but bonding with respect to C_1-C_1. Consequently, the calculated C_1-C_1 overlap population increases from 0.608 in free C_4H_6 to 0.818 in the coordinated ligand. In the limit of strong back-bonding, this central bond attains considerable double bond character, as illustrated by the canonical forms shown in Figure 4. The extent to which the bonding in any individual complex resembles either the 1−4-η-diene or enediyl forms clearly depends on the ability of the metal to give up electron density, stronger back-bonding causing a shift toward the enediyl form.

The disrotatory motion of the methylene protons has also been noted previously and interpreted in terms of the orientation of the C_4H_6 orbitals shown in Figure 3.[23] Disrotatory motion of the methylene protons directs the C_2 pπ orbitals inward toward the Ru center, thereby increasing the overlap of metal and ligand-based orbitals. In addition to the enhanced overlap described above, the 7a′ orbital of butadiene is also stabilized through in-phase overlap of the C_2 pπ orbitals, thereby increasing its electron-accepting ability. Similar distortions have been noted in a variety of coordinated hydrocarbon ligands and interpreted in an analogous fashion.[26] In order to determine the energetic significance of this disrotatory motion, we have reoptimized the structure of $Ru(PH_3)_3(C_4H_6)$ with all protons constrained to lie in the plane of the carbon backbone, thus preventing the distortion. The partially optimized structure has Ru−C bond lengths approximately 0.15 Å longer than those shown in Figure 2, indicating that the metal−ligand interaction is substantially reduced. The components of the total energy for the partially optimized structure, along with the population analysis, are compared to those of its fully optimized counterpart in Table 1. Clearly, the disrotatory motion of the protons dominates the preparation energy, some 30 kcal mol^{-1} being associated with the distortion, primarily due to the disruption of the ligand π system. This endothermic term is, however, more than compensated for by a much enhanced orbital interaction term when the protons are allowed to move out of the plane of the carbon framework. Furthermore, the difference in orbital interaction terms arises primarily from within the a′ representation, indicating that metal-to-ligand back-bonding is most strongly influenced by the rotation of the protons. Consistent with this hypothesis, the population analysis indicates that the major difference between the fully and partially optimized systems is a much reduced transfer of charge from metal to ligand in the latter. From a summation of the various components of the bonding energy, the net result of the disrotatory motion is a stabilization of the complex by 12.5 kcal mol^{-1}, approximately 20% of the total bond energy.

Linkage Isomerism in $Ru(PH_3)_3$(*o*-xylylene): Comparison of the Bonding at *exo* and *endo* Sites. Selected structural parameters from the optimized structures of both *endo* and *exo* isomers of $Ru(PH_3)_3$(*o*-xylylene) are presented in Table 2, along with that of the free ligand, C_8H_8. Parameters obtained from the X-ray structures of the *endo* and *exo* isomers of Ru$(PMe_2Ph)_3$(*o*-xylylene) are shown for comparison. The calculated metal−ligand bond lengths, Ru−C and Ru−P, are shorter than their experimentally determined counterparts, by between 0.02 and 0.10 Å. This behavior is typical of structures optimized using the local density approximation.[27] In contrast, the C−C bond lengths within the ligand framework are reproduced with remarkable accuracy, calculated values being within 0.025 Å of experiment in all cases. In accord with experimental findings, the carbon framework of the *exo* coordinated ligand is essentially planar, in marked contrast to the *endo* isomer, where the C_8 moiety is bent about the C_2-C_2 axis. However, close inspection of the coordinated C_4 units reveals that the nature of the structural distortion is in fact very similar in both cases. Just as in the butadiene system, the groups attached to the outer carbon centers undergo a disrotatory motion in order to attain maximum overlap with the metal center. In the *endo* isomer, this motion results in the displacement of the C_2-C_3 bond above the plane defined by the coordinated butadiene moiety and, hence, the

(26) Elian, M.; Chen, M. M. L.; Mingos, D. M. P.; Hoffmann, R. *Inorg. Chem.* **1976**, *15*, 1148−1155.
(27) Fan, L.; Ziegler, T. *J. Chem. Phys.*, **1991**, *95*, 7401−7408.

Downloaded by CARLI CONSORTIUM on June 30, 2009
Published on May 9, 1996 on http://pubs.acs.org | doi: 10.1021/om9600755

Table 2. Optimized Bond Lengths (Å) of *exo*-Ru(PH$_3$)$_3$(*o*-xylylene), *endo*-Ru(PH$_3$)$_3$(*o*-xylylene), and Free *o*-Xylylene

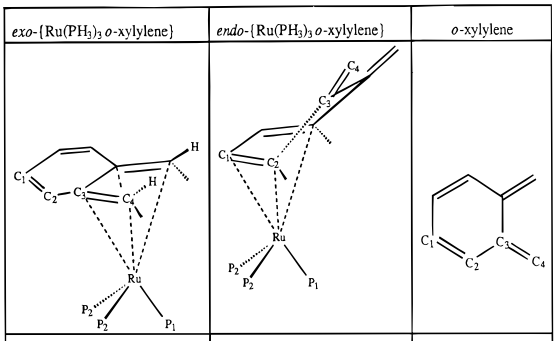

	exo-{Ru(PH$_3$)$_3$ o-xylylene}		endo-{Ru(PH$_3$)$_3$ o-xylylene}		o-xylylene
	Expt.[11]	Calc.	Expt.[7]	Calc.	Calc.
r(C$_1$-C$_1$)	1.394	1.403	1.384	1.408	1.432
r(C$_1$-C$_2$)	1.357	1.366	1.434	1.426	1.344
r(C$_2$-C$_3$)	1.420	1.414	1.460	1.453	1.441
r(C$_3$-C$_3$)	1.440	1.442	1.490	1.475	1.478
r(C$_3$-C$_4$)	1.436	1.433	1.327	1.336	1.346
r(Ru-C$_{3/1}$)	2.298	2.184	2.151	2.119	
r(Ru-C$_{4/2}$)	2.174	2.138	2.259	2.197	
r(Ru-P$_1$)	2.242	2.200	2.312	2.252	
r(Ru-P$_2$)	2.320	2.262	2.306	2.240	

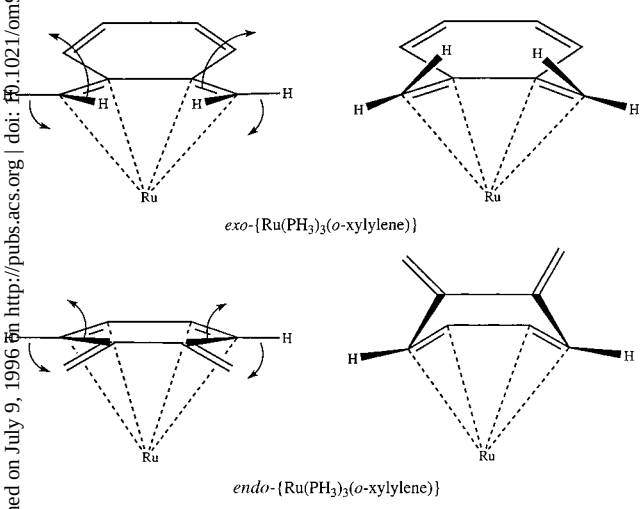

Figure 5. Consequences of the disrotatory motion at the terminal carbons in *exo*- and *endo*- Ru(PH$_3$)$_3$(*o*-xylylene).

marked nonplanarity of the C$_8$ fragment, as illustrated in Figure 5. In the *exo* isomer, the rotation involves only protons, just as in an isolated butadiene, and hence the carbon framework remains planar.

The components of the metal−ligand bond energy for the *exo* and *endo* isomers are summarized in Table 3, along with population analyses for the two isomers. From the total energies it is evident that the *exo* isomer is more stable than its *endo* counterpart by approximately 15 kcal mol^{-1}. The preference for *exo* coordination can be traced to the enhanced double-bond character of the central C−C bond in the coordinated ligand, illustrated in Figure 6. In the *exo* isomer, the central C−C bond is part of the six-membered ring, and consequently coordination of the metal fragment leads to an aromatization of the cyclic ring system. In contrast, coordination at the *endo* site results in no enhanced aromatization, and the two π systems are effectively isolated from each other by the approximately sp^3-hybridized C$_2$ centers. Overlap populations confirm

Table 3. Components of the Total Energy and Mulliken Population Analyses for *exo*-Ru(PH$_3$)$_3$(*o*-xylylene) and *endo*-Ru(PH$_3$)$_3$(*o*-xylylene)

Energy/kcal mol^{-1}

	endo	*exo*
ΔE_{prep}	27.60	37.86
ΔE_{st}	108.15	97.92
ΔE_{oi}		
a′	−147.18	−158.92
a″	−64.43	−67.28
corr[a]	7.26	6.36
ΔE_{tot}	−68.60	−84.06

Fragment Populations

	Ru(PH$_3$)$_3$	C$_8$H$_8$	Ru(PH$_3$)$_3$	C$_8$H$_8$
a′	18.40	23.60	18.30	23.70
a″	12.29	17.71	12.36	17.64
tot.	30.69	41.31	30.66	41.34

[a] Correction term accounting for the incomplete fit provided by the auxiliary functions.

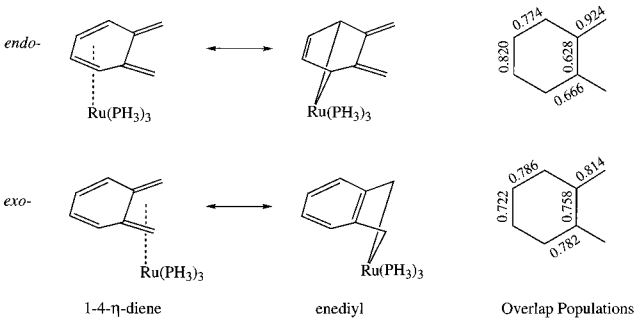

Figure 6. Canonical forms and overlap populations of *exo*- and *endo*-Ru(PH$_3$)$_3$(*o*-xylylene).

the aromatic character of the six-membered ring in the *exo* isomer, all six C−C bonds within the ring lying in the range 0.722−0.786, compared to a calculated value of 0.747 for benzene. Furthermore, the aromatization of the six-membered ring stabilizes the enediyl canonical form relative to the 1−4-η-diene alternative in the *exo* isomer. As a result, the bonds to the outer carbons (Ru−C$_4$) are appreciably shorter than those to the inner carbons (Ru−C$_3$) in the *exo* isomer, a situation typical of the enediyl coordination mode.[13f,g] In the *endo* isomer, the situation is reversed, and Ru−C$_1$ is shorter than Ru−C$_2$, a situation which is more typical of 1−4-η-diene coordination.[23−25] Similarly, in the *exo* isomer of Fe(CO)$_3$(*o*-xylylene), the bonds from the iron atom to the outer carbon atoms are shorter than those to the inner carbons, in contrast to the trend in other Fe(CO)$_3$-(1−4-η-diene) complexes.[28]

In addition to the electronic factors outlined above, there are also purely steric effects that disfavor the *endo* isomer. The optimized structures of the *endo* and *exo* isomers indicate that the displacement of the *anti* substituents above the plane of the carbon framework is substantially greater in the latter. The dihedral angle C$_3$−C$_3$−C$_4$-H$_a$ in the *exo* isomer is 55°, compared to a value of only 35° for the corresponding angle in the *endo* complex, C$_1$−C$_1$−C$_2$−C$_3$. The reason for this difference can be traced to the connectivity of the terminal carbon atoms involved in the disrotatory motion. In the *exo* isomer, the two terminal carbon atoms (C$_4$) are free to

(28) Batsanov, A. S.; Zol'nikova, G. P.; Struchkov, Yu. T.; Kritskaya, I. I. *Koord. Khim.* **1987**, *13*, 1551−1553; *Chem. Abs.* **1988**, *108*, 29808d.

Downloaded by CARLI CONSORTIUM on June 30, 2009
Published on July 9, 1996 on http://pubs.acs.org | doi: 10.1021/om960075

rotate without disturbing any other bonds in the molecule, just as they are in a simple butadiene complex (see Figure 5). In contrast, the two rotating termini (C_2) in the *endo* isomer are linked *via* the C_3-C_3 single bond; consequently the disrotatory motion can only be accomplished at the expense of increased strain elsewhere in the molecule. In this case, the C_2-C_3 bond is longer than in the free ligand, and there is also a substantial distortion of the $C_1-C_2-C_3$ angle away from 120°. As noted above, the principal effect of the disrotatory motion is to enhance the metal-to-ligand back-bonding, and the population analyses summarized in Table 3 confirm that this feature of the bonding is indeed more prominent in the *exo* isomer than in its *endo* analogue.

Conclusions

In this paper we have shown that the metal−ligand bonding in butadiene complexes is dominated by back-bonding from metal to ligand, which accounts for approximately 70% of the total interaction energy. Approximately 20% of this total arises because of a displacement of the methylene protons out of the C_4 plane, thereby increasing the overlap of metal- and ligand-based orbitals and also stabilizing the ligand LUMO. The donation of electron density into the ligand LUMO generates partial double-bond character at the central C−C bond, causing a distinct contraction of this bond relative to the free ligand. The principles described for the bonding in simple butadiene complexes can be extrapolated to account for the different stabilities of the *endo* and *exo* isomers of $Ru(PH_3)_3$(*o*-xylylene). The increase in central C−C bond order upon coordination results in an aromatization of the six-membered ring in the *exo* isomer only. The stabilization of the enediyl canonical form of the *exo* isomer as a result of this aromatization is reflected in the Ru−C bond lengths of the two systems. In the *endo* isomer, the bonds to the central carbon atoms are shorter than those to the outer atoms, whereas the opposite trend applies in the *exo* form, as it does in structurally characterized enediyl systems. The relative stability of the *endo* isomer is further reduced by the restricted rotation of the outer carbon atoms caused by the constraints of the six-membered ring. As noted for the simple butadiene complex, this disrotatory motion can account for up to 20% of the total bond energy and, hence, the restriction may be a significant factor in reducing the stability of the *endo* isomer.

OM9600755

Downloaded by CARLI CONSORTIUM on June 30, 2009
Published on July 9, 1996 on http://pubs.acs.org | doi: 10.1021/om9600755